Smart material and design solutions for protective headgears in linear and oblique impacts

Column/matrix composite liner to mitigate rotational accelerations

Mosleh, Y.; Cajka, Martin; Depreitere, Bart; Ivens, Jan; Vander Sloten, Jos

DOI
10.1088/1361-665X/aca575

Publication date
2022

Document Version
Final published version

Published in
Smart Materials and Structures

Smart material and design solutions for protective headgears in linear and oblique impacts: column/matrix composite liner to mitigate rotational accelerations

To cite this article: Yasmine Mosleh *et al* 2023 *Smart Mater. Struct.* **32** 014001

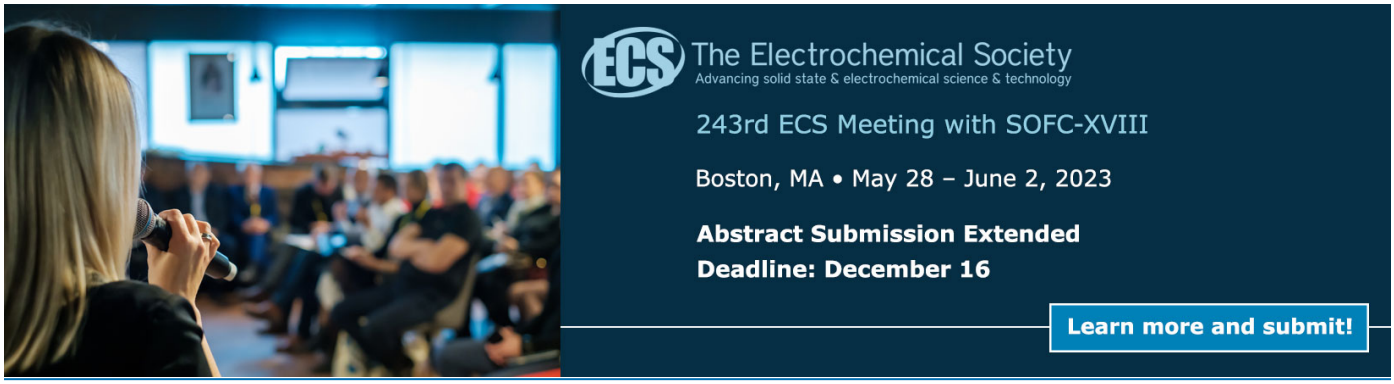

OPEN ACCESS
IOP Publishing
Smart Materials and Structures
Smart Mater. Struct. **32** (2023) 014001 (15pp)
https://doi.org/10.1088/1361-665X/aca575

Smart material and design solutions for protective headgears in linear and oblique impacts: column/matrix composite liner to mitigate rotational accelerations

Yasmine Mosleh[1,*], Martin Cajka[2], Bart Depreitere[3], Jan Ivens[4] and Jos Vander Sloten[5]

[1] Department of Engineering Structures, Faculty of Civil Engineering and Geosciences, TU Delft, Delft, The Netherlands
[2] Department of Applied Mechanics and Mechanical Engineering, TU Kosice, Kosice, Slovakia
[3] Department of Neurosurgery, University Hospital Gasthuisberg, KU Leuven, Leuven, Belgium
[4] Department of Materials Engineering, KU Leuven, Leuven, Belgium
[5] Department of Mechanical Engineering, KU Leuven, Leuven, Belgium

E-mail: Y.Mosleh@tudelft.nl

Received 12 July 2022, revised 26 October 2022
Accepted for publication 23 November 2022
Published 5 December 2022

Abstract

Oblique impact is the most common situation that cyclists experience during traffic accidents during which the human head undergoes both linear and rotational (angular) accelerations. Angular acceleration of the head is known to be linked to the majority of traumatic brain injuries. This paper proposes various solutions to mitigate angular accelerations of which an anisotropic column/matrix composite foam design is the most effective. This smart design allows tailor-made adjustment of shear and compressive resistance of the foam liner. Regarding helmet shells, tough fiber-reinforced composite materials such as self-reinforced polypropylene (PP) (Curv®) and silk/high-density polyethylene (HDPE) were benchmarked against conventional brittle polycarbonate (PC). Results demonstrate the superior performance of silk/HDPE composite compared to PC in resisting perforation in localized impact involving sharp objects. Regarding the helmet liner, two configurations were studied particularly, a multi-layered and column/matrix design. Their efficacy was benchmarked against single-layer homogenous expanded polystyrene (EPS) foam of equivalent weight and thickness in linear and oblique impact using experimental and finite element methods. The results showed the superior behavior of the column/matrix configuration. Such smart design could be combined with other smart systems such as multi-directional impact protection system (MIPS) technology for possible synergy and enhanced performance in head protection.

Keywords: head protection, composite shell, composite foam, oblique impact, helmet design

(Some figures may appear in colour only in the online journal)

* Author to whom any correspondence should be addressed.

1. Introduction

Cyclists are some of the least protected road traffic participants. Head injuries are the most common injury types that a cyclist undergoes in a traffic accident and helmets are the sole protection system for a cyclist against head injuries during a traffic accident. The protective effect of bicycle helmets in minimizing head and brain injuries is acknowledged in various epidemiological, experimental, and computational studies [1–6].

In real life, cyclists often experience oblique impacts [7]. Oblique impacts give rise to both linear (translational) and rotational (angular) accelerations of the head. Rotation of the head is linked to traumatic brain injuries e.g. contusions, subdural hematoma (SDH), and diffuse axonal injury (DAI) [8–10]. However, the effectiveness of cycling helmets is mainly evaluated by measuring linear accelerations using a vertical drop test on a flat anvil. Current cycling helmet test standards do not include a rotational acceleration in their pass/fail criteria [11].

These test standards such as CPSC 1203, EN 1078, AS/NZS 2063, and CSA-D113.2-M89 are similar in certifying helmets for preventing penetrating injuries to the head, reducing skull-brain relative motion, and keeping biomechanical injury criteria within human injury tolerance. However, the impact energy thresholds in these standards vary depending on the drop height [11].

Increased awareness of the effect of rotational acceleration in traumatic brain injuries has sparked extensive research for coming up with anti-rotational helmet design technologies e.g. based on a slip-layer that is placed inside the helmet such as multi-directional impact protection system (MIPS) [12], 6D helmet [13], and shearing pad inside (SPIN) [14]. Also different collapsible structures were proposed to replace expanded polystyrene (EPS) liner, examples of which are Wavecel helmet [15], and Koroyd helmet [16]. Moreover, anisotropic foams were proposed to directly replace conventional isotropic foams as helmet liners [17–19]. The hypothesis is that by introducing anisotropy in a foam liner [20, 21] with the direction of anisotropy perpendicular to the head surface, the shear stresses transmitted to the head can be reduced, and by limiting the tangential force transferred to the head, the rotational movement of the head can be reduced.

Another design concept particularly for equestrian helmets focuses on varying foam density through the thickness by combining layers with different densities or functionally graded foams. Preliminary impact simulations, only evaluated for linear acceleration, suggest that using layered or functionally graded foams in helmets could improve impact absorption and reduction in peak linear accelerations for low and medium impact velocities (4.4 m s^{-1}–5.4 m s^{-1}) [22–24].

In a helmet, the outer shell also plays a crucial role. The function of the outer shell is to distribute the impact energy over a larger area, prevent penetration of sharp objects, and to absorb some part of the impact energy. Another function of the outer shell is enabling the helmet to slide on the road, thus minimizing tangential forces which cause neck injury. In commercial bicycle helmets, a very thin shell made of materials such as thermoplastic polymer such as polycarbonate (PC), acrylonitrile-butadiene-styrene copolymer, or polymer composite (e.g. glass fiber reinforced polymer) is used [25]. Some researchers evaluated the performance of woven fabric composite shells such as carbon, glass, and Kevlar composite using finite elements (FEs) and concluded that the composite materials can help to reduce peak accelerations of the head, and the Kevlar sample out-performed others due to its low shear strength and stiffness [26, 27].

This paper investigates various design solutions to improve the performance of cycling helmets to mitigate linear and rotational accelerations during linear and oblique impacts. Anisotropic composite foam liners in two configurations of 'layered' (with varying foam density through the thickness) and 'column/matrix' designs are studied using both experimental and numerical methods. For this, actual experiments were performed on flat foam specimens by placing them on flat and 45° anvils and dropping a Hybrid III dummy head of a 50th percentile male, while collecting and benchmarking the accelerations experienced by the head for different foam configurations. Both experimental and numerical results demonstrate that the composite foam with column/matrix configuration should be proposed as the optimum solution to mitigate head injuries during linear and oblique impacts.

Furthermore, the effect of the helmet shell material on the helmet performance in linear impact by blunt and sharp projectiles is studied at room temperature. For this study, tough thermoplastic fiber reinforced composites namely self-reinforced polypropylene (PP) (CURV®), and silk/high-density polyethylene (HDPE) composite were chosen and benchmarked against brittle PC shells.

2. Materials

2.1. Helmet shell material and production method

The effect of helmet shell thickness and material type have been studied by performing drop weight impact on cuboids of EPS foam with a density of 60 kg m^{-3} covered with shell material. For investigating the effect of materials type, three different shell materials namely PC sheet, self-reinforced PP composite (CURV®), and Silk/HDPE composite with a thickness of around 1.5 mm were investigated. For studying the effect of shell thickness, PC shells with two different thicknesses of 0.5 and 1.5 mm were prepared and subsequently tested in linear impact.

PC sheets with a thickness of 0.5 mm and 0.75 mm were sourced from the helmet manufacturing company Lazer Sport in Belgium. PC shell with a thickness of 1.5 mm was produced by compression molding of two PC sheets with a thickness of 0.75 mm at a temperature of 200 °C and by applying a pressure of 15 bar for 5 min. Then samples were subsequently cooled to 90 °C. After 15 min holding time at 90 °C the samples were cooled to room temperature and removed from the hot press.

CURV® composite shells with an average thickness of 1.4 mm, were obtained from Propex Fabrics (Germany).

Another composite shell chosen for this study was a silk/HDPE composite. A silk twill woven fabric with an areal weight

Table 1. Different shell materials and their thicknesses.

Shell sample code	Material type	Thickness (mm)
PC 0.5	Polycarbonate	**0.48 ± 0.05**
PC 1.5	Polycarbonate	**1.49 ± 0.02**
Curv	Self-reinforced polypropylene composite	**1.39 ± 0.01**
Silk/HDPE	Composite of silk twill weave/high density polyethylene	**1.50 ± 0.03**

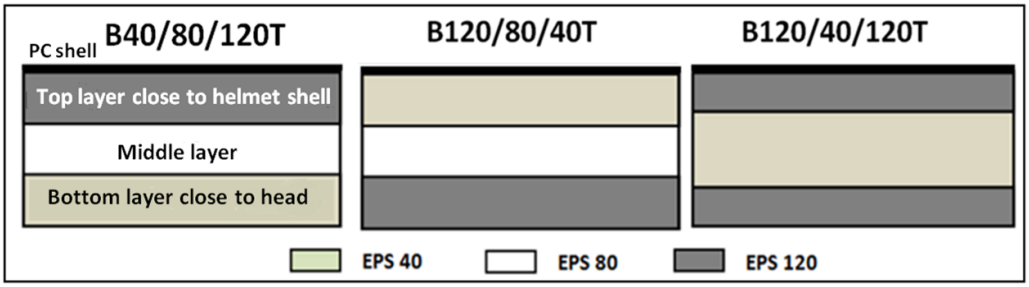

Figure 1. Illustration of different configurations of composite foams composed of layers of EPS40 (density of 40 kg m^{-3}), EPS80 (density of 80 kg m^{-3}), and EPS120 (density of 80 kg m^{-3}), from left to right, B40/80/120T; B120/80/40T, and B120/40/120T, respectively, where B is the bottom location near the head and T is the top position adjacent to the helmet shell and all these three layered composite foam samples have the overall thickness of 24 mm and overall density of 80 kg m^{-3}.

of 80 g m^{-2} was sourced from the company Hermes, France. To prepare silk/HDPE composite shells, high-density polyethylene modified with maleic anhydride (HDPE-MA), Bynel 40×10^{529}, in the form of a film with a thickness of 0.065 mm was supplied by Du Pont. The thermoplastic silk/HDPE composite shells were produced by compression molding using a hot press (Fontijne). The processing temperature was set at 150 °C. The applied pressure was set to 15 bar for 8 min. Then samples were cooled to 90 °C. After 15 min holding time at 90 °C, the samples were cooled to room temperature and removed from the hot press. Fiber volume fraction of silk fiber in the composite plate was around 50%. The sample code of the different shells and their actual thickness are listed in table 1.

2.2. Multi-layer EPS foam liner

Multi-layer liners were prepared by combining discrete layers of EPS foam with three different densities of 40 ± 3, 80 ± 3, and 120 ± 4 kg m^{-3}, EPS40, EPS80, and EPS120, respectively. EPS foams were sourced from Kemisol and Lazer Sport in the shape of blocks with a thickness of 24 mm.

Three different configurations used in this study namely B120/80/40T, B40/80/120T, and B120/40/120T are illustrated in figure 1. As illustrated in figure 1, e.g. B120/80/40T refers to the configuration where higher density foam (EPS120), is close to the head or impact projectile and EPS40 is adjacent to the helmet shell. Overall density and thickness of all three configurations were aimed at 80 kg m^{-3} and 25 mm, respectively. To achieve the overall density of 80 kg m^{-3} for EPS40/80/120 layered composite foams, all three layers of EPS40, EPS80, and EPS120, were cut into the thickness of 8 mm. For cutting the foam layers, a hot wire was used to ensure a smooth surface. In the EPS120/40/120 configuration, for achieving an overall density of 80 kg m^{-3}, EPS120 and EPS40 layers were cut into a thickness of 6 and 12 mm, respectively, to obtain an overall density of 80 kg m^{-3}. Single-layer EPS80 was considered as the reference material to which the performance of multi-layer foams is compared. EPS80 is used prevalently as a liner in commercial bicycle helmets.

3. Experimental methods

3.1. Linear impact testing of different shells

Two different projectiles were used for impacting the different shells which are shown in figures 2(a) and (b). Figure 2(a) demonstrates a steel flat tub with a diameter of 50 mm and a steel finger projectile with a hemispherical tip and diameter of 16 mm for applying localized loads as shown in figure 2(b). The drop height and weight were set at 1.5 m and 4.5 kg respectively, resulting in an impact velocity of 5.4 m s^{-1}. This is the velocity suggested by the current European bicycle helmet standard, EN 1078 [28].

For preparing samples for impact tests on different shells, first, the shells were cut and glued to EPS60 foam cuboids with the dimension of 100 mm × 100 mm × 24 mm using double-sided adhesive tape Kip® 342 as illustrated in figure 2(c). Impact tests were performed using a drop tower impactor. Instead of gluing the samples to the impact tub, they were clamped between two heavy steel rings with an opening of 70 mm, as shown in figure 2(d). The bolts on the ring were tightened carefully by applying the same amount of torque 20 N m on every bolt to avoid misalignment, using a torque meter.

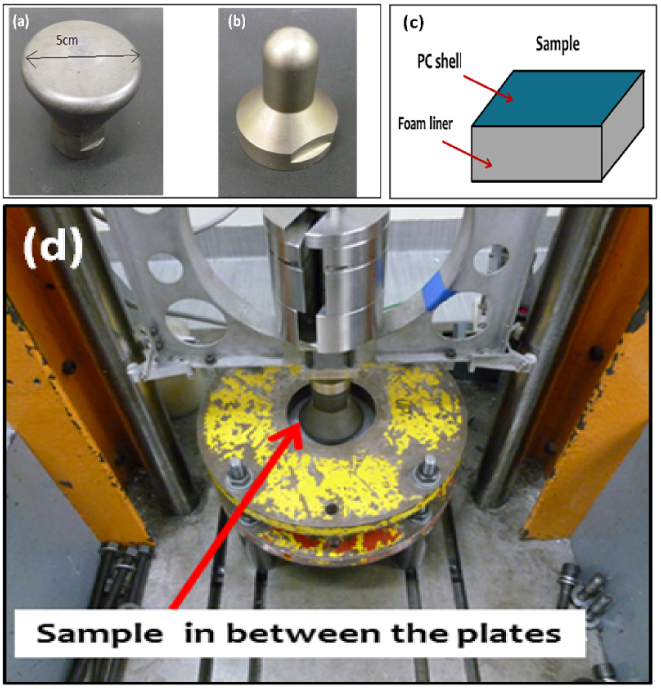

Figure 2. Projectiles used in drop weight impact experiments on different shells (a) steel flat tube with a circular cross-section of 5 cm diameter; (b) steel finger projectile with 16 mm diameter. (c) Illustration of a foam specimen covered with PC shell used for impact testing. (d) An example of a foam sample covered with a shell fixed in between two steel rings with an opening of 70 mm in the drop impact tower and impacted by a flat steel tub.

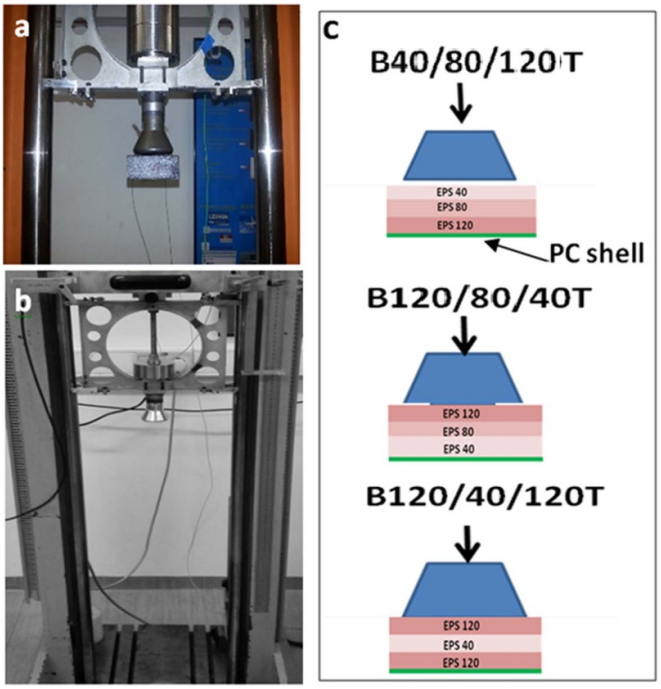

Figure 3. (a), (b) Drop weight impact tower; (c) illustrations of three configurations of composite foams connected to flat steel tub.

3.2. Compression tests of foam liners

Quasi-static tests were performed according to ASTM standard D1621/94 using a universal tensile testing machine (Instron 4467). Foams were compressed at a constant displacement rate of 2.4 mm min^{-1} between two parallel steel plates. The displacement and the load were recorded. Samples were cut into cuboids of 50 mm (length) × 50 mm (width) × 24 mm (thickness). All the tests were performed at room temperature and repeated at least three fold.

3.3. Linear impact tests of foam liners

Linear impact tests on foam samples were performed using a drop-weight impact tower set-up equipped with a flat steel projectile, which is shown in figures 3(a) and (b). The circular cross-section of the steel projectile has a radius of 50 mm and it is attached to a frame. The total drop weight was set at 4.5 kg resembling the average weight of a Hybrid III dummy head of a 50th percentile male that is used in oblique impact experiments. The drop height was fixed at 1.5 m resulting in an impact velocity of 5.4 m s^{-1}. Force applied to the projectile during impact was monitored by a Kistler load cell, type 9041 A; displacement was monitored with a laser sensor. Foam specimens were prepared in the form of cuboids with dimensions of 70 mm (length) × 70 mm (width) × 24 mm (thickness) and taped to the projectile using double-sided adhesive tape (Kip® 342). As illustrated in figure 3(c), a PC shell with a thickness of 0.5 mm was also taped to the outer surface of each foam liner specimen using the same double-sided tape.

3.4. Oblique impact of foam liners

An illustration of the oblique impact set-up used in this study is shown in figure 4. In this set-up, a Hybrid III dummy head of a 50th percentile male is utilized as the headform and is incorporated into the existing drop weight impact tower. The head was supported by grips, shown in figure 4(b), until the moment that the head impacts the anvil. This was to ensure that the Hybrid III headform remains oriented at 45° during free fall onto the anvil. The grips are mounted on the rails of the drop tower impact set-up. Also, a high speed camera was used to monitor the head orientation and it was observed that the head remains at the same orientation, and any rotation of the head prior to impact was minimal. An array of three linear accelerometers and a gyroscope in the center of gravity of the dummy head allows the measurement of the three linear accelerations and three rotational velocities in x, y, and z directions, respectively. Rotational velocities about three directions of x, y and z (ωx ωy ωz), are measured by an IES 3103 triaxial angular rate sensor with an angular rate measurement range up to 4800° s^{-1} (or 83.7 rad s^{-1}). For the measurement of linear accelerations in directions of x, y, and z, three uniaxial MEMS 64C-2000-300 accelerometers with a measurement range of 0–2000 g were utilized. To obtain the results, a sampling rate of 7000 Hz was used. Signals were subsequently filtered offline in MATLAB using a second-order Butterworth filter with a cut-off frequency of 175 Hz.

The head was fixed at a height of 1.5 m resulting in an impact velocity of 5.4 m s^{-1}. An anvil with an angle of 45°

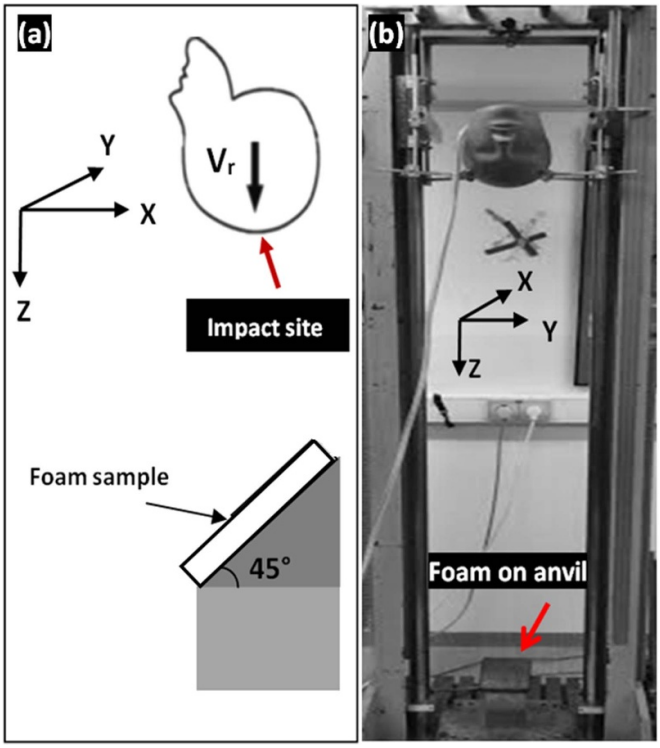

Figure 4. Illustration of oblique impact set up equipped with hybrid III dummy head which falls on the foam sample at an impact angle of 45°, the drop direction is shown by a black arrow; sample laid on 45° anvil is shown by the red arrow, (a) side view and (b) front view.

was used for the oblique impact test. Foam samples in the shape of cuboids and dimensions of 80 mm (length) × 80 mm (width) × 24 mm (thickness) were glued firmly on the 45° anvil as shown in figure 3(b). The head was subsequently dropped on the sample.

All materials were tested at least three times to ensure the repeatability of the results and a representative curve has been chosen for the interpretation of the results. All experiments were performed at room temperature.

3.5. Global head injury criteria

The oblique impact test results are subsequently analyzed according to global head injury criteria such as HIC (linear head injury criterion) and RIC (rotational head injury criterion), for a more relevant analysis of the results.

The HIC is the most common head injury indicator that accounts for both the magnitude and duration of linear acceleration [29]. The HIC formula is presented in equation (1), in which the measured linear acceleration, $a(t)$, is in g's (9.81 m s^{-2}) and t is in seconds. The time interval $t_2 - t_1$ is limited to 15 ms which gives HIC_{15} values [30],

$$\mathrm{HIC} = \left\{ \left({}^{1}/_{(t_2 - t_1)} \int_{t_1}^{t_2} a(t) \right)^{2.5} (t_2 - t_1) \right\}_{\max}. \qquad (1)$$

The RIC was proposed in the same form as HIC and is described by equation (2), in which $\boldsymbol{\alpha(t)}$ stands for resultant rotational acceleration in rad s^{-2} and t is in seconds [31],

$$\mathrm{RIC} = \left\{ \left({}^{1}/_{(t_2 - t_1)} \int_{t_1}^{t_2} \alpha(t) \right)^{2.5} (t_2 - t_1) \right\}_{\max}. \qquad (2)$$

4. Modeling description

The FE impact simulation of physical oblique impact consists of three main parts: the EPS foam, the headform, and the anvil. The impact simulations were carried out for two different impact velocities of 5.4 m s^{-1} and 6.5 m s^{-1}. For the simulation of oblique impact behavior, two different configurations were considered which are shown in figure 5. In the first case, the flat foam sample with dimensions of 8 cm (length) × 8 cm (width) × 2.5 cm (thickness) is placed on a 45° anvil and the headform is dropped vertically on the foam specimen with the specified impact velocities. In the second configuration, the foam is placed on the spherical headform and covers half of the spherical headform, resembling a hemispherical helmet which is illustrated in figures 5(b) and (c).

The headform is subsequently dropped on the 0° and 45° anvil simulating linear or oblique impact, respectively. For simplification, the headform is approximated as a sphere. The radius of the spherical head model was set at 8.5 cm. The weight of the headform was set to 4.5 kg similar to the weight of a hybrid III dummy head. In these simulations, the headform is modeled as a rigid body and the linear and rotational accelerations transferred to the headform are measured from the center of mass.

The EPS foam liner was modeled in Abaqus/Explicit using the crushable foam model for isotropic material with volumetric hardening in conjunction with a linear elastic model. Material properties of EPS crushable foams such as Young's modulus, yield stress, and plateau stress for the constitutive model used in the current study were determined by performing quasi-static compression experiments. The strain hardening in EPS foam is s a function of strain rate. For defining parameters for incorporating strain rate dependency in the material model, linear impact tests on EPS foams were used as input [32]. Further detail on the foam material model can be found in the recent paper of the authors [32]. The Poisson's ratio of EPS is considered equal to zero in these simulations.

For meshing of the foam, C3D8R elements (linear brick elements) were used with distortion control which does not allow elements to invert during large deformations.

The anvil was also modeled as an analytically rigid part. The friction coefficient between the headform and the foam in the configuration where the foam was placed on the anvil (figure 5(a)) and also between the hemispherical helmet and the anvil (figures 5(b) and (c)) was set to $f = 0.3$. The foam was connected to the anvil, in figure 1(a), or to the headform, in figure 1(b), using coupling where all the degrees of freedom of the foam surface which was in contact with the anvil or with the headform were restrained. This simplification was chosen because the emphasis of this study was on comparing different configurations of the EPS foam, relative to each other.

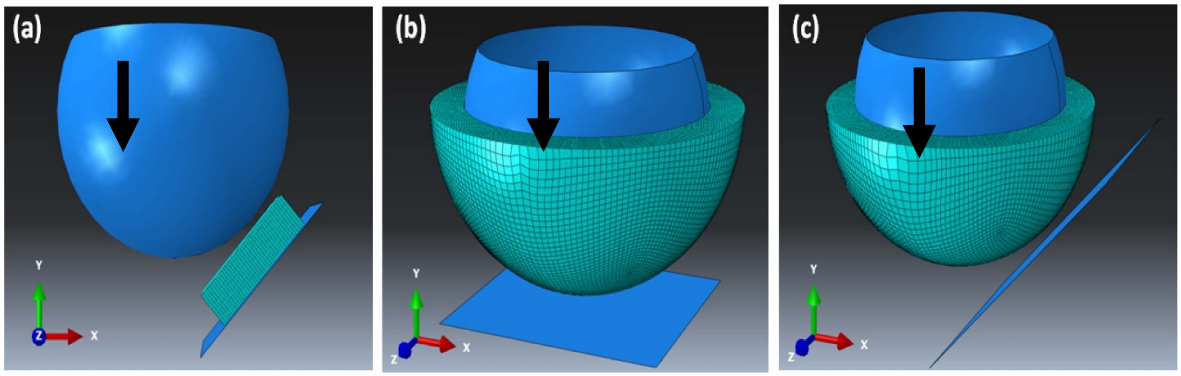

Figure 5. Illustrations of (a) oblique impact of the head on a foam where the foam sample is placed on an anvil at an angle of 45°; (b) linear impact of helmeted head on the anvil at the angle of 0°; (c) oblique impact of the helmeted head at an angle of 45°, the black arrow demonstrates the direction of the impact velocity.

5. Results and discussions

5.1. Experimental results

5.1.1. Effect of shell material on impact performance of the helmet. Linear impact tests were performed on different shells with two projectiles, a steel finger projectile (figure 6(a)) and a steel flat projectile (figure 6(b)) to see the effect of local shell deformation on the impact results.

As shown in figures 7(a)–(d), during the impact tests using the steel finger projectile all the foam samples covered with PC shells (both thicknesses of 0.5 and 1.5 mm) and Curv® shells were perforated, except for the samples with silk/HDPE composite shell. This is due to the higher penetration impact resistance of silk/HDPE composite. The combination of tough silk fibers (with strain to failure of 20%) and a thermoplastic matrix such as HDPE-MA with high strain to failure (820%) leads to higher deformability and a better spread of the damage in the composite shell, avoiding localization and perforation at this impact velocity. Previous research carried out by several researchers on penetration resistance of glass and carbon fiber-reinforced composites indicated that the fiber volume fraction was the dominant factor controlling penetration impact and that the matrix type had no noticeable effects [33, 34]. However, other researchers demonstrated the crucial effect of the matrix on the impact resistance of composites reinforced with tough fibers (e.g. tough stainless steel and silk fibers) [35–38]. The reason could be that during impact, tough fibers surrounded by a matrix with a high strain to failure, can still fail first and, thus, their toughness can be exploited to its full potential. Impact results on different shells indicate the importance of a suitable tough composite shell in protecting the head against perforation by sharp objects which is more probable in e.g. the case of mountain biking.

During the impact tests using the steel flat projectile, none of the shells were punctured. All samples except for PC0.5 showed a similar peak force and impact time duration. As observed in figure 6(b) and within the limited test range, the thickness of PC shells plays a dominant role in peak force/acceleration which can be related to lower bending stiffness of PC0.5 allowing for larger deformation between the projectile and the sample (see figures 7(e) and (f)).

5.1.2. Compression and linear impact experiments on layered foams. The compressive stress–strain curves of multi-layer composite foams EPS40/80/120, and EPS120-40-120 versus single-layer EPS80, obtained from quasi-static compression experiments, are plotted in figure 8(a). It can be observed that layered EPS foams demonstrate a step-wise behavior in compression. For EPS40/80/120, the compressive stress–strain curve comprises three stress plateaus; each of which relates to a different density layer. The first stress plateau is related to the yielding of the EPS40 layer and the second plateau stress is the result of the yielding of the EPS80 layer. Finally, the EPS120 layer undergoes compression loading. EPS120-40-120 composite foam sample demonstrates two plateaus in the compressive stress–strain curve attributed to EPS40 and EPS120 layers, respectively. In general in multi-layer foam, when the layers are loaded in series, the number of steps that appear in the stress–strain curve is equal to the number of different densities in the configuration. In addition, the length of each plateau region is directly related to the thickness of the corresponding layer. In the helmet application, it is important that the foam liner can absorb the energy while keeping the stress below the injurious level. The magnitude of compressive stress is correlated with acceleration. To compare the energy absorption efficiency of layered EPS liner with single layer EPS80, figure 8(b) shows absorbed energy density versus stress for each configuration. It can be observed that the multi-layer foams initially demonstrate a gradual tendency to absorb energy while the single-layer EPS80, does not dissipate energy before the stress of 0.78 MPa. However, after the stress level of 0.78 MPa, EPS80 outperforms the layered foams in energy absorption at intermediate stress levels. It is believed that the analysis of energy absorption efficacy of the foams in quasi-static compression can be a good indication of the behavior of the foam in dynamic linear impact inside a helmet.

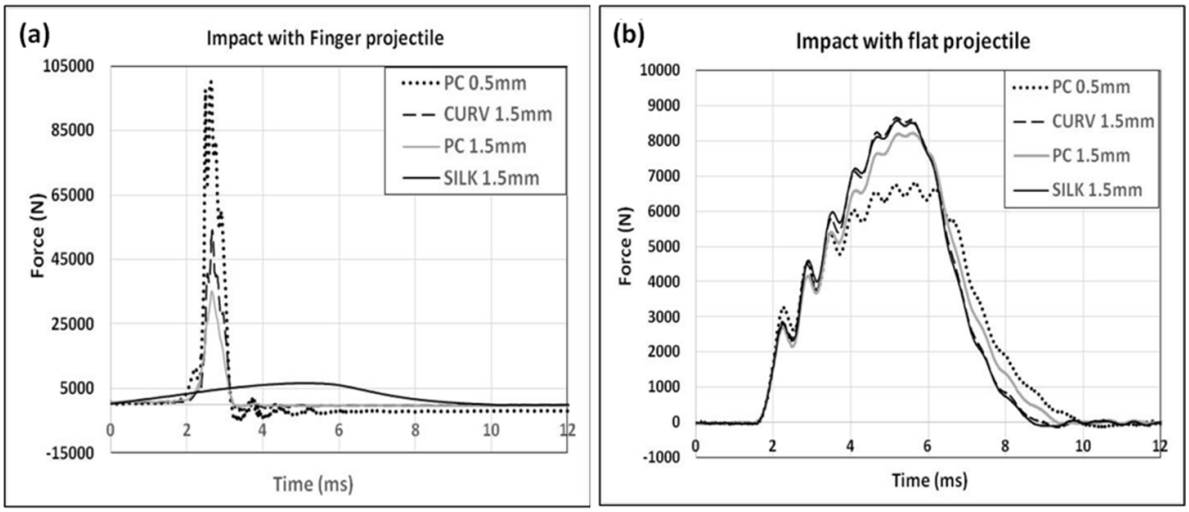

Figure 6. Linear impact force-time graphs with (a) finger steel tub and, (b) flat steel tub. High peak forces lead to high peak accelerations which should be avoided.

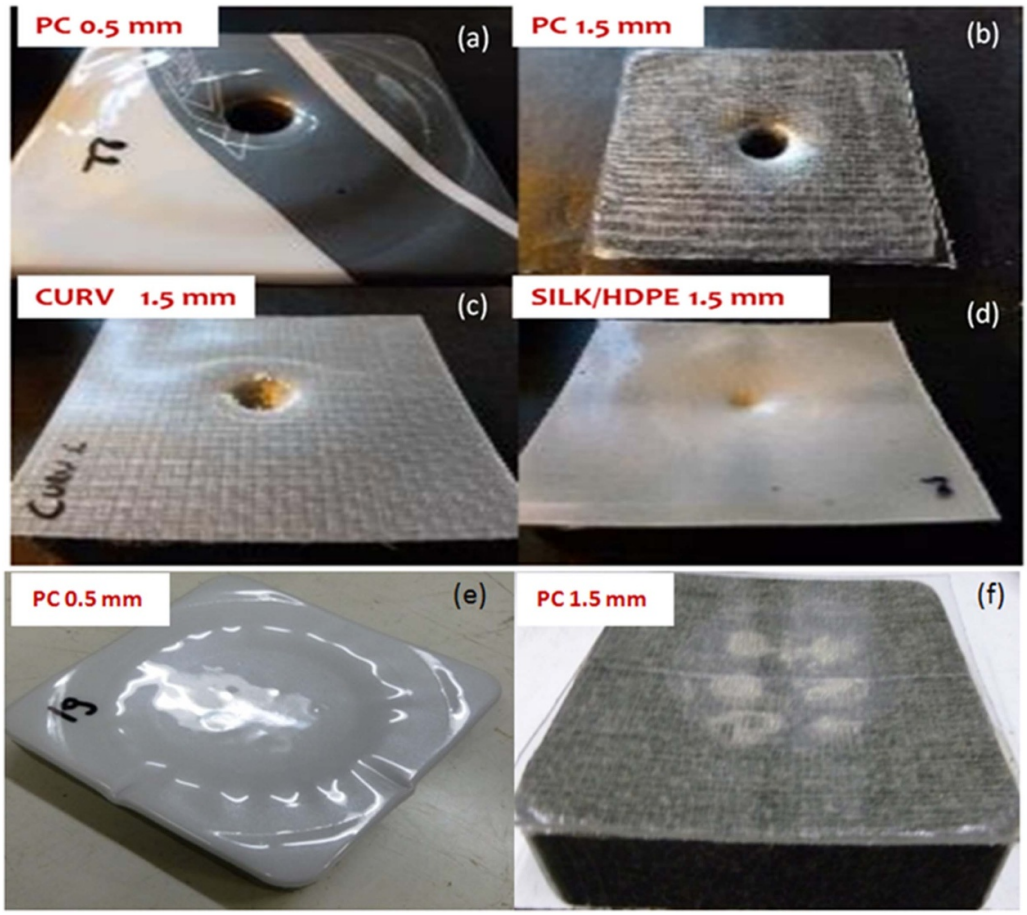

Figure 7. Perforated samples of EPS foam covered with (a) PC shell with a thickness of 0.5 mm, (b) PC shell with a thickness of 1.5 mm, (c) self-reinforced PP (CURV) shell, (d) silk/HDPE composite shell, impacted by steel finger projectile with an impact velocity of 5.4 m s^{-1}; samples of EPS foam covered with (e) PC shell with a thickness of 0.5 mm, (f) PC shell with a thickness of 1.5 mm, impacted by flat steel projectile at a velocity of 5.4 m s^{-1}.

To evaluate this hypothesis, the linear impact was performed on all three configurations of layered foam and compared with EPS80. A linear drop weight impactor was used for this purpose as shown earlier in figure 3.

As shown in figure 8(c), the layered EPS foam liners demonstrate higher force (accelerations) levels than EPS80. This is in line with the findings of energy density versus stress graphs (figure 8(b)). The initial energy recommended

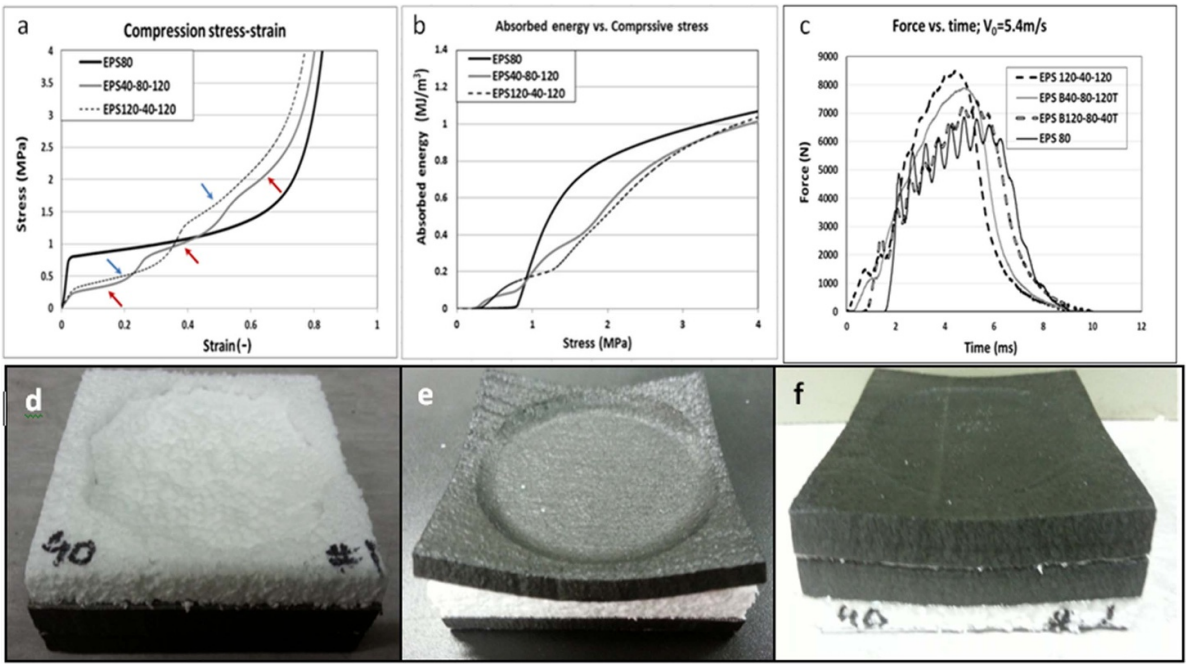

Figure 8. (a) Stress–strain curves of layered composite foams versus EPS80 obtained from quasi-static compression test; (b) comparative curves of absorbed energy versus compressive stress for layered composite foams and EPS80; (c) force-time curves of layered foams versus EPS80, obtained from drop weight impact experiments with an impact velocity of 5.4 m s^{-1}; (d)–(f) impacted samples of B40/80/120T, B120/40/120T, and B120/80/40T respectively.

for testing bicycle helmets according to EN 1078 (considering the acceleration limit of 250 g and approximate head weight of 5 kg) is much higher than the observed threshold of 0.18 MJ m^{-3}. The detailed calculations can be found in chapter 6 of the PhD thesis of Vanden Bosche [38]. Therefore, it is believed that the layered foam liners can demonstrate superior impact protection in helmets, only at low impact energies. Another interesting observation is that the configuration of the layered EPS foam, particularly the sequence of the different density layers, affects the impact performance. As observed, by placing the higher density foam layer close to the head in the case of EPSB120/80/40T, the foam liner can absorb the energy in lower force/acceleration levels in comparison to EPSB40/80/120T. This can be attributed to the fact that placing lower density foam close to the head leads to a more concentrated load due to its weaker compressive properties. In contrast, by placing the higher density layer close to the head in the gradient, the load further spreads and a less localized load can be seen in figures 8(d) vs. (f). The highest peak force is related to EPSB120/40/120T. A possible explanation can be related to the higher thickness of the EPS40 layer, in this case, in comparison to the gradient configurations of EPSB120/80/40T and EPSB40/80/120T to achieve a similar overall density of 80 kg m^{-3}. At the moment of impact, lower density EPS40 is the first layer that deforms and enters the densification region. This leads to a higher portion of overall thickness that is densified when the EPS120 layers take over the load. The thicker densified region causes EPSB120/40/120T to act as a foam of higher density in the higher stress range and overall the material experiences higher force/acceleration levels, as is observed in figures 8(a)–(c).

In conclusion, there seems to be a correlation between the energy absorption ability of different layered EPS foams in compression tests and during linear impact. Also, it can be concluded that layered EPS foam liner can outperform single-layer EPS foam, with similar overall density, only in low energy impacts and when higher density foam is positioned adjacent to the head.

5.1.3. Experimental oblique impact. The performance of multi-layered EPS foam liner versus EPS80, when impacted at an oblique angle of 45° was investigated. For this, flat foam specimens were placed on the 45° anvil, and the hybrid III dummy head was subsequently dropped on the foam samples with an impact velocity of 5.4 m s^{-1}. Figures 9(a)–(c) demonstrates the resultant linear and rotational accelerations and rotational velocity versus time of multi-layer foams in comparison to EPS80. As observed, peak linear accelerations of layered EPS liners are similar to EPS80 except for EPSB120/80/40T, which can be related to a less localized impact loading. Slight prolongation of the impact duration can also be observed in the layered foams which can be related to the stepwise deformation in layered foam, starting in the softer layers, which can prolong the contact time between the head and foam specimen. Layered EPS foam liners demonstrated lower peak rotational acceleration in comparison to EPS80. The lower rotational acceleration and lower rotational velocity slope can be related to the lower shear stresses transmitted to the head in the earlier stages of contact. Easier shear deformation of the EPS40 layers in the layered foam structures can lead to a reduction of shear stress transfer to the head and hence lower rotational acceleration values. However, it is

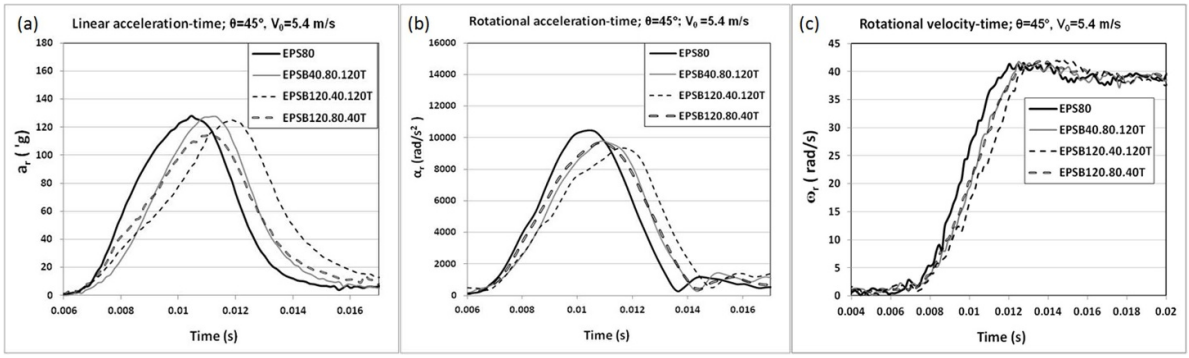

Figure 9. Oblique impact behavior of three different configurations of layered composite foam versus EPS80 obtained from oblique impact experiments in which flat foam specimens are placed on an anvil at 45° and are impacted by the dummy head at an impact velocity of 4.5 m s^{-1}, (a) resultant linear acceleration-time, (b) rotational acceleration-time, and (c) rotational velocity-time.

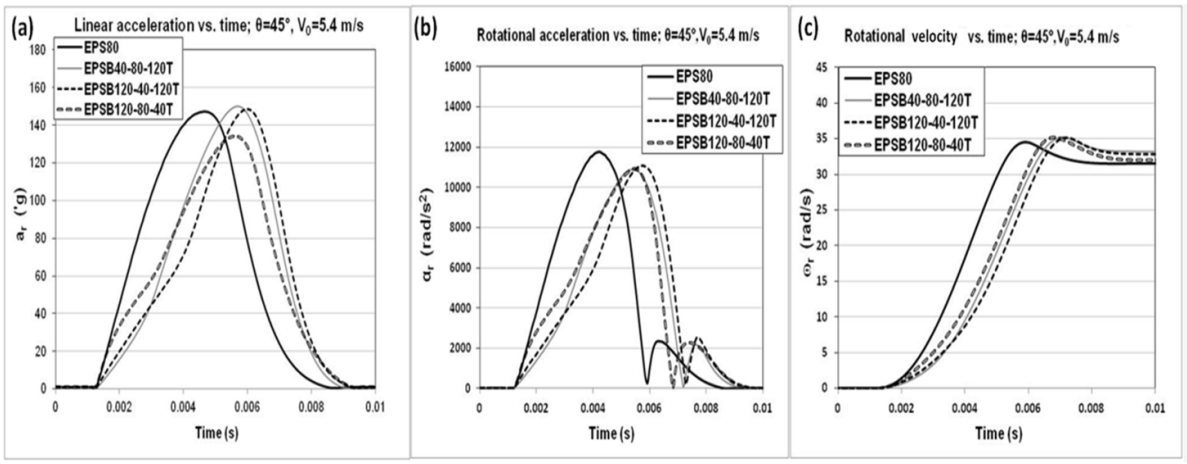

Figure 10. Simulated oblique impact behavior of three different configurations of layered composite foam versus EPS80 obtained from oblique impact experiments in which flat foam specimens are placed on an anvil at 45° and are impacted by the dummy head at impact velocity of 4.5 m s^{-1}, (a) resultant linear acceleration-time, (b) rotational acceleration-time, and (c) rotational velocity-time.

believed that for higher impact energies, the soft layer densifies leading to the higher shear resistance of the structure. This is further investigated by numerical modeling in the following sections.

5.2. Impact simulation results

The linear and oblique impact simulations of spherical headforms are presented (see figure 5). In one case the spherical head is dropped on multi-layered and single-layer EPS foam and linear and rotational accelerations transferred to the head form during impact are presented. In another case, the head form is covered with foam resembling a helmet. The purpose of this section is to first assess the eligibility of the current numerical simulations for evaluation of the performance of different foam configurations in linear and oblique head tests, which can save time and labor of actual experimentation. Secondly, a qualitative comparison will be done of different layered EPS configurations versus single-layer EPS as a helmet foam material. It is interesting to investigate the performance of a helmet by inducing a gradient density through the foam liner thickness, without changing the overall thickness or weight.

5.2.1. Oblique impact simulations of flat foam samples. Figures 10(a)–(c), respectively, shows the calculated linear and rotational accelerations and rotational velocity versus time of multi-layer composite foams in comparison to EPS80. In these simulations, the foams were placed on the 45° anvil and the spherical headform dropped on the foam specimens with an impact velocity of 5.4 m s^{-1}.

By comparing figures 9(a)–(c) and 10(a)–(c), it can be concluded that there is a good agreement between experimental and simulation results in terms of predicting the relative behavior of the different configurations of multi-layer composite foams with respect to each other and to EPS80. The shape of the linear and rotational acceleration versus time and rotational velocity versus time curves are very similar to the results obtained from the experiments. All the layered composite foams show lower rotational acceleration values and also a lower slope of the rotational velocity, for the used impact velocity of 5.4 m s^{-1}. Moreover, EPSB120/80/40T seems to be the best configuration since it also transfers lower linear acceleration levels in comparison to EPS80, as was also observed during the experiments. In both simulation and experimental results, a prolongation of impact duration around

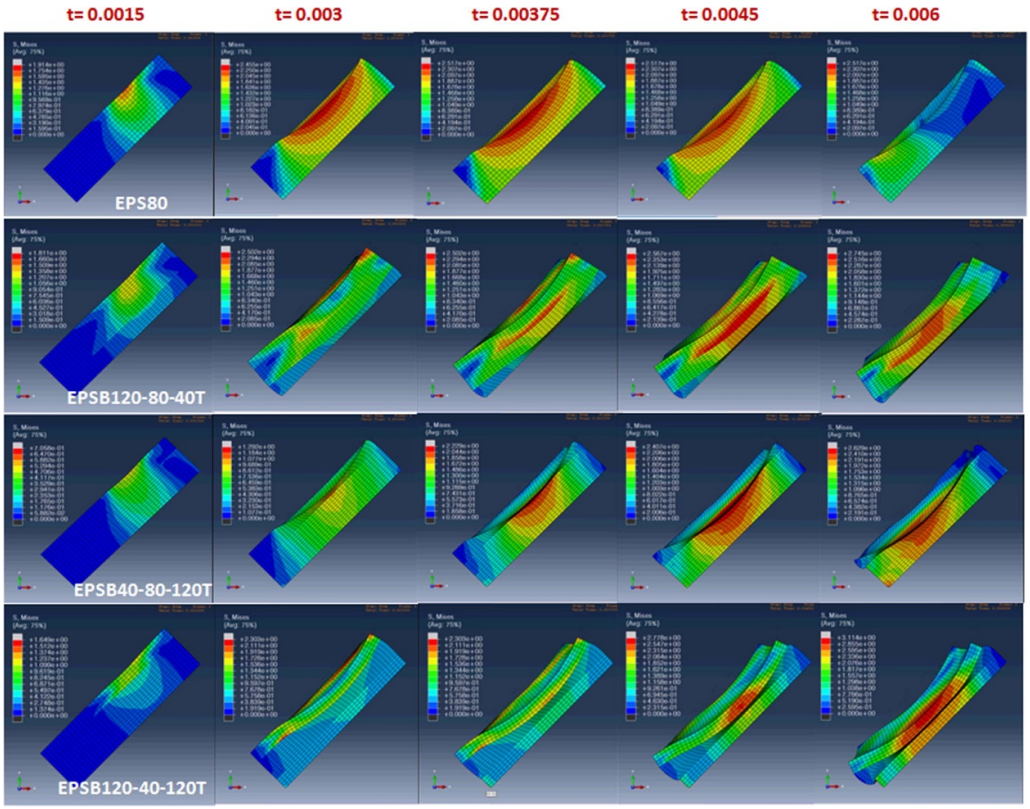

Figure 11. The evolution of deformation of EPS80 foam and layered EPS foams with time during oblique impact (impact velocity of 5.4 m s^{-1}) is shown by snapshots from simulations.

2 ms can be seen for multi-layer foams in comparison to EPS80. As mentioned earlier this could be due to the stepwise deformation in the layered foam. In layered foams deformation starts in the softer layers which can be observed in figure 11, in which evolution of deformation in different layered foams is shown with the progression of time.

However, absolute values of linear and rotational acceleration and velocity in simulation curves show slightly higher values compared to experimental curves. One of the reasons for this discrepancy in absolute peak values between simulations and experimental curves can be that the simulated head form is approximated as a sphere whilst in actual experiments in this study a hybrid III dummy head was used. Another reason could be the different friction coefficient between the dummy head and the foam (covered by a comfort pad) during experiments than the value of 0.3 that was assumed in the model since friction can affect rotation. However, due to a lack of data on the value of the friction coefficient, this cannot be further scrutinized.

5.2.2. Linear impact simulations of helmeted heads. Figures 12(a) and (b) demonstrates the linear acceleration versus time curves obtained from linear impact simulations of helmeted heads with impact speeds of 5.4 and 6.5 m s^{-1}, respectively. It can be seen that the numerical results are in line with the conclusion which was drawn from compression and linear impact experimental results (figure 8). Multi-layer EPS liners demonstrate higher peak linear acceleration in comparison to EPS80. For both impact velocities of 5.4 and 6.5 m s^{-1}, it can be observed that the highest peak acceleration is related to the EPSB120/40/120T configuration, which is believed to be related to the thicker layer of EPS40 which densifies before the higher density layers and leads to a bigger ratio of the densified layer in comparison to other configurations. Similar to observations in drop weight impact experiments on flat samples, it can be seen that the configuration where the higher density layer is closer to the head transfers lower accelerations to the head, however, it cannot outperform EPS80.

5.2.3. Oblique impact simulations of a helmeted head. Figures 13(a)–(c) demonstrates the linear and rotational accelerations and rotational velocity transmitted to the headform whilst impacting the 45° anvil, with an impact velocity of 5.4 m s^{-1}. As observed, for the impact velocity of 5.4 m s^{-1}, the EPSB120/80/40T helmet transfers slightly lower peak linear and rotational accelerations to the head compared to the EPS80 helmet while EPSB120/40/120T and EPSB40/80/120T helmets show similar peak linear and rotational accelerations to EPS80 helmet. These results are somewhat different from the experiments and simulations of flat foam samples; in that case, all layered foam samples showed reduced rotational acceleration.

In addition, in the helmeted head simulations, all the layered EPS foam configurations demonstrate a lower slope before reaching peak accelerations for both linear and

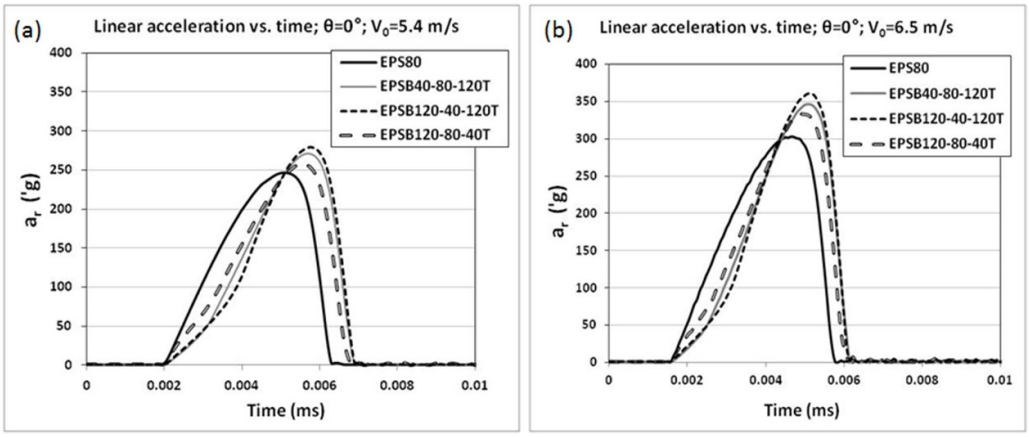

Figure 12. Simulated performance of helmets made of layered composite foam in linear impact in comparison to EPS80 reference helmet at an impact velocity of (a) 5.4 m s^{-1}, and (b) 6.5 m s^{-1} (a_r is resultant linear acceleration).

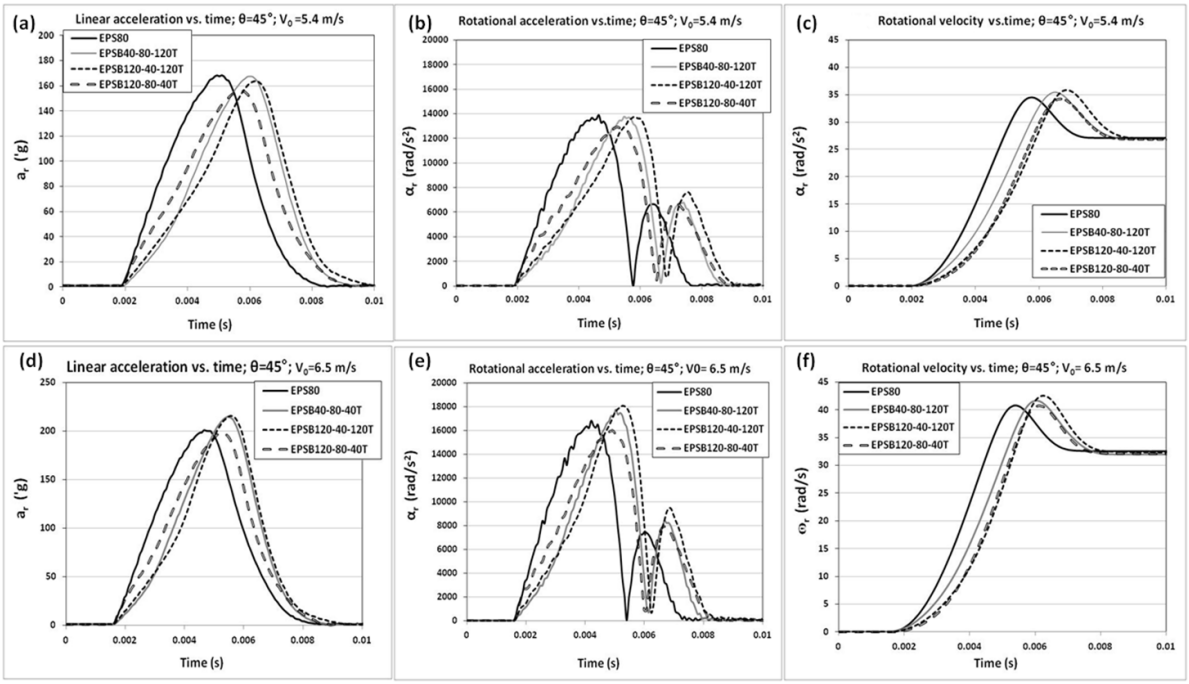

Figure 13. Simulated performance of helmets made of three different configurations of layered composite foams versus EPS80 obtained from FE simulations of oblique impact at an angle of 45° and two impact velocities of 5.4 and 6.5 m s^{-1}; (a) and (d) resultant linear acceleration–time, (b) and (e) rotational acceleration–time, and (c) and (f) rotational velocity–time.

rotational accelerations and prolongation of the impact duration by around 2 ms, compared to EPS80. This can be related to the weaker EPS40 layers in layered foams. However, at a higher impact velocity of 6.5 m s^{-1}, as shown in figures 12(d)–(f), EPS80 demonstrates lower linear and rotational acceleration peaks than the layered foam configurations, except for EPSB120/80/40T. As shown earlier in figures 12(a) and (b), in linear impact, EPS80 outperforms all three layered EPS foam configurations.

The values for peak linear and rotational acceleration for impact velocities of 5.4 and 6.5 m s^{-1} and both linear and oblique impacts, from simulations on helmeted heads, are tabulated in table 2.

5.2.4. Analysis of the data based on global injury criteria. To avoid concluding the performance of multi-layer foam solely based on peak acceleration and to take into account pulse duration, the test results are analyzed according to global head injury criteria such as linear HIC, and RIC. The calculated HIC and RIC values for linear and oblique impacts are tabulated in table 3. As shown in table 3, in linear impact the helmets with the layered configurations demonstrate higher HIC values than standard EPS80 helmets for both impact velocities of 5.4 and 6.5 m s^{-1}. However, in oblique impact, for an impact velocity of 5.4 m s^{-1}, HIC values for layered foam and specifically the EPS120B-80-40T material show slightly lower values than EPS80, and also for an impact velocity of 6.5 m s^{-1}, only the

Table 2. Tabulated values of peak resultant linear ($a_{r,max}$) and rotational accelerations (α_{rmax}) and peak rotational velocity (ω_{max}), from simulations on helmeted heads, for both layered foams and EPS80 for impact angles of 0° and 45° and two impact velocities of 5.4 and 6.5 m s^{-1} .

	$V_0 = 5.4$ m s^{-1} $\theta = 0°$	$V_0 = 6.5$ m s^{-1} $\theta = 0°$	$V_0 = 5.4$ m s^{-1} $\theta = 45°$			$V_0 = 6.5$ m s^{-1} $\theta = 45°$		
Sample code	$a_{r,max}$ (g)	$a_{r,max}$ (g)	$a_{r,max}$ (g)	$\alpha_{r,max}$ (rad s^{-2})	ω_{max} (rad s^{-1})	$a_{r,max}$ (g)	$\alpha_{r,max}$ (rad s^{-2})	ω_{max} (rad s^{-1})
EPS80	246	300	141	13 600	34.4	200	16 836	40.8
EPSB40/80/120T	270	346	142	13 775	35.4	182	17 562	41.5
EPSB120/40/120T	278	360	140	13 731	35.8	186	18 053	42.5
EPSB120/80/40T	258	333	133	12 863	34.1	200	15 951	40.7

Table 3. Calculated values with HIC and RIC for different layered composite foam configurations versus EPS80.

	$V_0 = 5.4$ m s^{-1} $\theta = 0°$	$V_0 = 6.5$ m s^{-1} $\theta = 0°$	$V_0 = 5.4$ m s^{-1} $\theta = 45°$		$V_0 = 6.5$ m s^{-1} $\theta = 45°$	
Sample code	HIC_{15}	HIC_{15}	HIC_{15}	RIC	HIC_{15}	RIC
EPS80	100%	100%	100%	100%	100%	100%
EPSB40/80/120T	122%	138%	94%	92%	99%	101%
EPSB120/40/120T	127%	145%	86%	89%	103%	103%
EPSB120/80/40T	106%	130%	84%	89%	91%	93%

EPS120B-80-40T helmet can slightly outperform the EPS80 helmet.

As can be observed in table 3, at an impact velocity of 5.4 m s^{-1}, the calculated RIC values for the multi-layer composite are slightly lower than for the EPS80 helmet. The decrease in RIC values in the case of the EPSB120/80/40T Prototype is up to 10%. For an impact velocity of 6.5 m s^{-1}, only the EPSB120/80/40T helmet exhibits a lower RIC value than the EPS helmet (8.5%).

From simulation results, it can be concluded that multi-layer foams cannot outperform single-layer EPS foam of the equivalent weight and thickness in linear impact. In oblique impact, results of simulation for an impact velocity of 5.4 m s^{-1} show that layered composite helmets can outperform EPS80 helmets, however for a higher impact velocity of 6.5 m s^{-1}, only the EPSB120/80/40T helmet can slightly outperform the EPS80 helmet by reducing peak linear and rotational accelerations. However, no clear change in peak rotational velocity by using multi-layer composite helmets was observed.

Concluding, both the simulation results and the earlier experimental results indicate that no significant benefits for impact energy absorption may be expected from layered foam liner configurations, notwithstanding some positive reports in the literature [22–24]. However, instead of using layered foam configurations which are loaded in series during impact, as an alternative, parallel-loaded composite foam configurations were evaluated, which turned out to give very clear reductions in rotational acceleration [18, 32].

5.3. Proposition of column/matrix configuration as the optimum solution

A composite foam concept comprising two different densities of EPS foams in a 'column/matrix' configuration is proposed as illustrated in figure 14. Matrix foam was chosen from a lower density foam, more precisely foam with lower shear and compressive resistance e.g. EPS40 whilst EPS120 was chosen for the columns. The direction of mechanical anisotropy in the composite foam configuration is in the z direction (through the thickness). This means in case such a structure is used as a helmet liner, the direction of anisotropy would be perpendicular to the surface of the head as illustrated in figure 14. Here, "EPS40m/EPS120f/5 × 5" stands for a composite foam sample with EPS60 as the matrix foam and EPS120 as column foam with 25 columns arrayed in a square packing. More information on fabrication, and parameters affecting the properties of the column/matrix composites is presented in previous research papers [18, 19, 32].

Table 4 summaries the resultant linear and rotational accelerations, rotational velocity, HIC_{15} and RIC criteria for the column/matrix configuration versus single layer EPS80 flat foam samples when the headform impacted a flat foam specimen laid on the anvil at an angle of 45° with impact velocity of 5.4 m s^{-1}. It can be concluded that the composite foam concept can reduce linear and rotational accelerations as well as the rotational velocity and injury criteria in comparison to a single layer. This further confirms the hypothesis that by creating anisotropy, rotational acceleration transmitted to the head can be reduced without change in the weight and thickness of the liner [18, 19, 39].

The values for peak linear and rotational accelerations, and rotational velocity obtained from oblique impact (45°) simulations of helmeted head for both impact velocities of 5.4 and 6.5 m s^{-1} are tabulated in table 5.

The composite foam helmet with a foam column (fiber) diameter of 5.8 mm shows a reduction in HIC values of around 20%. Moreover, composite foam helmets could have half the RIC value, showing the merit of the composite concept in specifically reducing rotational acceleration.

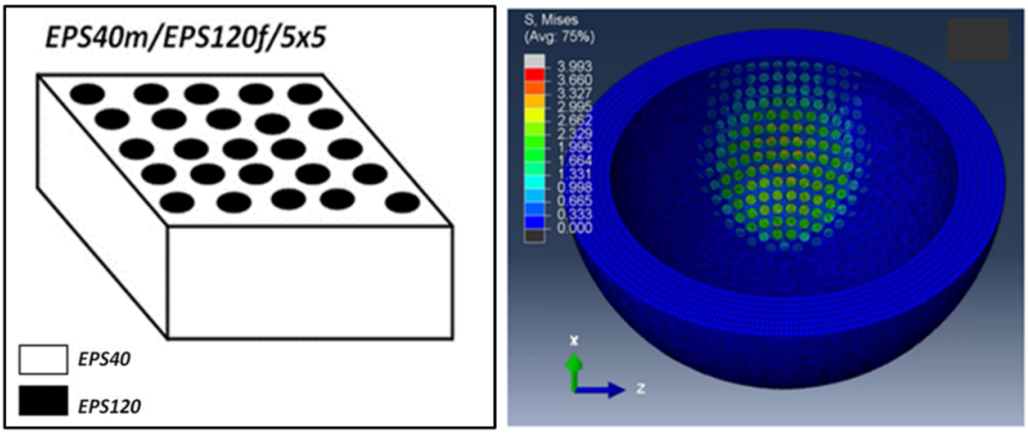

Figure 14. Illustration of 'column ('fibre')/matrix' composite foams, flat sample configuration (left), and simulated helmet configuration (right).

Table 4. Peak linear and rotational accelerations, and rotational velocity obtained from oblique impact (45°) simulations and calculated values of HIC, RIC, criteria composite foams vs. EPS80 at impact velocities of 5.4.

Sample code	a_{max} (g)	α_{max} (rad s^{-2})	ω_{max} (rad s^{-1})	HIC_{15}	RIC
EPS80 Reference	123 ± 2	10 400 ± 400	40.0 ± 1.0	402 ± 18	16 870 ± 100
EPS40m/EPS120f/5 × 5	106 ± 2	5780 ± 300	32.5 ± 0.5	328 ± 2	5910 ± 400

Table 5. Tabulated values of peak linear and rotational accelerations and rotational velocity obtained from oblique impact (45°) simulations and calculated values of HIC, RIC, criteria composite foams vs. EPS80 at impact velocities of 5.4 and 6.5 m s^{-1}.

Helmet code	V_0, (m s^{-1})	a_{max} (g)	α_{max} (rad s^{-2})	ω_{max} (rad s^{-1})	HIC_{15}	RIC
EPS80	5.4	168	13 900	34	673	19 500
	6.5	200	16 800	39.6	1051	30 300
Helmet EPS40m/EPS120f	5.4	144%–14%	10 177%–27%	29%–15%	529%–21%	9826%–50%
	6.5	178%–12%	14 000%–17%	35.5%–10%	840%–20%	16 306–46%

To sum up, it can be concluded that the column/matrix composite liner design similar to other anti-rotational helmet systems presented in literature can contribute to the simultaneous reduction of linear and rotational accelerations, compared to the conventional EPS helmet [11]. All these earlier mechanisms of anti-rotational helmet designs have aimed at the reduction of rotational acceleration whilst simultaneously absorbing impact energy and linear accelerations. These anti-rotational concepts such as a slip-layer could be combined smartly with the currently proposed composite foam liner for possible synergistic effects. The column/matrix design in itself allows for a smart design of the foam liner, because it is possible to steer the relative compressive and shear resistance, with the volume fraction of the columns, their slenderness (diameter) and the densities of the two foam materials.

6. Conclusions

This paper comprises two main parts. In the first part, the effect of helmet shell material and thickness on the impact resistance of a helmet against blunt and sharp projectiles was studied by performing drop weight impact tests. For this, composite shells of self-reinforced PP and silk/HDPE were benchmarked against conventional PC shells. The results indicate that only a tough composite of silk/HDPE can protect the helmets against perforation by sharp projectiles. Moreover, it was observed that using a thinner PC shell could lead to lower peak accelerations upon loading with a flat projectile, attributed to lower bending stiffness which allows for higher deformability.

In the second part of this paper, multi-layer EPS with three different configurations was prepared and their compression and impact performance was compared with single-layer EPS of similar thickness and weight. Results from compression experiments showed that the multi-layer foams initially absorb the energy more efficiently, however, after a certain stress level (in case of our material around 0.78 MPa), single layer EPS80 outperformed composite foams by absorbing more energy at intermediate stress levels. In the next step, the performance of multi-layer foams as a helmet liner in linear and oblique impact was investigated via FE simulations. Results demonstrated that the multi-layer composite foam with equal thickness and overall density did not outperform the single layer EPS80 foam in linear impact for both impact velocities of 5.4 and 6.5 m s^{-1} which are relevant velocities for bicycle

helmet testing. In oblique impact, only the EPSB120/80/40T configuration in which the high density EPS120 layer is the closest to the head can slightly outperform EPS80 based on the peak acceleration values and HIC and RIC calculations. Based on the results of this paper, notwithstanding earlier positive reports in literature, it seems multi-layer configurations are merely an equal alternative for single layer foam with the same density and thickness when protection as a helmet liner is targeted.

Finally, composite foams with a column/matrix configuration are proposed as a substitute for single-layer EPS foam of equivalent weight and thickness for head protection, aiming at the reduction of rotational movement of the head during oblique impacts. The experimental and numerical oblique impact results demonstrated the superior efficacy of the column/matrix composite foam concept which can be used as a smart structural solution for producing safer helmets that can further mitigate rotational accelerations and velocity. This concept can also be used in combination with other smart helmet design systems which specifically aim at mitigation of the head rotational movement such as MIPS, for a possible synergy. Moreover, the column/matrix design in itself allows for a smart design of the foam liner, due to the possibility of steering the relative compressive and shear resistance, with the volume fraction of the columns, their slenderness (diameter), and the densities of the two foam materials.

It should be noted that the oblique impact experiments in this study were performed only on the top of the Hybrid III head (figure 4). It is possible that the effectiveness of these materials is dependent not only on impact velocity but also on impact location relative to the head. Another important aspect to be noted is that, in the current study, the experimental results from impacts involving the 50th percentile male Hybrid III dummy head were compared with computational results from FE simulations involving an idealized spherical head. These limitations can be additional aspects to further scrutinize in future studies.

Data availability statement

All data that support the findings of this study are included within the article (and any supplementary files).

Acknowledgments

Authors wish to thank Flemish research funding agency, FWO, for the support of this research through the Project OT-Levenslijn (G.0C67.13).

ORCID iD

Yasmine Mosleh https://orcid.org/0000-0002-7322-1539

References

[1] Thompson D C, Rivara F and Thompson R 1999 Helmets for preventing head and facial injuries in bicyclists *Cochrane Database Syst. Rev.* CD001855
[2] Attewell R G, Glase K and McFadden M 2001 Bicycle helmet efficacy: a meta-analysis *Accid. Anal. Prev.* **33** 345–52
[3] Olivier J and Creighton P 2017 Bicycle injuries and helmet use: a systematic review and meta-analysis *Int. J. Epidemiol.* **46** 278–92
[4] Hoye A 2018 Bicycle helmets-to wear or not to wear? A meta-analyses of the effects of bicycle helmets on injuries *Accid. Anal. Prev.* **117** 85–97
[5] McIntosh A S, Lai A and Schilter E 2013 Bicycle helmets: head impact dynamics in helmeted and unhelmeted oblique impact tests *Traffic Inj. Prev.* **14** 501–8
[6] Fahlstedt M, Halldin P and Kleiven S 2016 The protective effect of a helmet in three bicycle accidents—a finite element study *Accid. Anal. Prev.* **91** 135–43
[7] Bourdet N, Deck C, Serre T, Perrin C, Llari M and Willinger R 2014 In-depth real-world bicycle accident reconstructions *Int. J. Crashworthiness* **19** 222–32
[8] Depreitere B, Van Lierde C, Maene S, Plets C, Van der Sloten J, Van Audekercke R, Van der Perre G and Goffin J 2004 Bicycle-related head injury, a study of 86 cases *Accid. Anal. Prev.* **36** 561–7
[9] Gennarelli T A and Thibault L E 1982 Biomechanics of acute subdural hematoma *J. Trauma* 22 680–6
[10] Gennarelli T A, Thibault L E, Adams J H, Graham D I, Thompson C J and Marcincin R P 1982 Diffuse axonal injury and traumatic coma in the primate *Ann. Neurol.* **12** 564–74
[11] Leng B, Ruan D and Tse K M 2022 Recent bicycle helmet designs and directions for future research: a comprehensive review from material and structural mechanics aspects *Int. J. Impact Eng.* **168** 104317
[12] MIPS (available at: https://mipsprotection.com/) (Accessed 20 November 2022)
[13] 6D Helmets (available at: www.6dhelmets.com/) (Accessed 20 November 2022)
[14] Bottlang M, Rouhier A, Tsai S, Gregoire J and Madey S M 2020 Impact performance comparison of advanced bicycle helmets with dedicated rotation-damping systems *Ann. Biomed. Eng.* **48** 68–78
[15] Bliven E, Rouhier A, Tsai S, Willinger R and Bourdet N 2019 A novel strategy for mitigation of oblique impacts in bicycle helmets *J. Forensic Med.* **10** 1 (available at: https://koroyd.com/)
[16] Vanden Bosche K, Mosleh Y, Depreitere B, Vander Sloten J, Verpoest I and Ivens J 2017 Anisotropic polyethersulfone foam for bicycle helmet liners to reduce rotational acceleration during oblique impact *Proc. Inst. Mech. Eng.* H **231** 851–61
[17] Mosleh Y, Vander Sloten J, Depreitere B and Ivens J 2017 Novel composite foam concept for head protection in oblique impacts *Adv. Eng. Mater.* **19** 1700059
[18] Mosleh Y, Pastrav L, Van Vuure A W, Depreitere B, Vander Sloten J and Ivens J 2018 Optimization of composite foam concept for protective helmets to mitigate rotational acceleration of the head in oblique impacts: a parametric study *Adv. Eng. Mater.* **20** 1700443
[19] Mosleh Y, Van den Bosche K, Depreitere B, Vander Sloten J, Verpoest I and Ivens J 2017 Effect of polymer

foam anisotropy on energy absorption during combined shear-compression loading *J. Cell. Plast.* **54** 597–613
[20] Mosleh Y, Depreitere B, Vander Sloten J and Ivens J 2018 Decoupling shear and compression properties in composite polymer foams by introducing anisotropy at macro level *J. Reinf. Plast. Compos.* **37** 657–67
[21] Cui L, Kiernan S and Gilchrist M D 2009 Designing the energy absorption capacity of functionally graded foam materials *Mater. Sci. Eng.* A **507** 215–25
[22] Forero Rueda M A, Cui L and Gilchrist M D 2009 Optimisation of energy absorbing liner for equestrian helmets. Part I: layered foam liner *J. Mater. Des.* **30** 3405–13
[23] Cui L, Forero Rueda M A and Gilchrist M D 2009 Optimisation of energy absorbing liner for equestrian helmets. Part II: functionally graded foam liner *Mater. Des.* **30** 3414–9
[24] Di Landro L, Sala G and Olivieri D 2002 Deformation mechanisms and energy absorption of polystyrene foams for protective helmets *Polym. Test.* **21** 217–28
[25] Fortis A P, Milis Z, Kostopoulos V, Tsantzalis S, Kormas P, Tzinieris N and Boudouris T,2002 Finite element analysis of impact damage response of composite motorcycle safety helmets *Injury* **33** 489–93
[26] Cernicchi A, Galvanetto U and Iannucci L 2008 Virtual modelling of safety helmets: practical problems *Int. J. Crashworthiness* **13** 451–67
[27] CEN EN 1078 1997 Helmets for pedal cyclists and for users of skateboards and roller skates (Brussels: Comité Européen de Normisation, European Committee for Standardization)
[28] Versace J 1971 A review of the severity index *15th Stapp Car Crash Conf.* pp 771–96
[29] Eppinger R and Takhounts E G 2000 Supplement: development of improved injury criteria for the assessment of advanced automotive restraint systems (II) *Stapp Car Crash J.* **44** 51–57
[30] Kimpara H and Iwamoto M 2012 Mild traumatic brain injury predictors based on angular accelerations during impacts *Ann. Biomed. Eng.* **40** 114–26
[31] Mosleh Y, Cajka M, Depreitere B, Vander Sloten J and Ivens J 2018 Designing safer composite helmets to reduce rotational accelerations during oblique impacts *Proc. Inst. Mech. Eng.* H **232** 479–91
[32] Caprino G and Lopresto V Factors affecting the penetration energy of glass fibre reinforced plastics subjected to a concentrated transverse load *Proc. 9th European Conf. on Composite Materials (ECCM-9)*
[33] Caprino G and Lopresto V 2001 On the penetration energy for fibre-reinforced plastics under low-velocity impact conditions *Compos. Sci. Technol.* **61** 65–73
[34] Van Vuure A W, Vanderbeke J, Osorio L, Trujillo E, Fuentes C and Verpoest I 2009 Natural fibre composites: tough silk and strong bamboo *Proc. 17th Int. Conf. on Composite Materials (ICCM-17)* (*Edinburgh*)
[35] Van Vuure A W, Vanderbeke J, Mosleh Y, Verpoest I and El-Asmar N 2021 Ductile woven silk fibre thermoplastic composites with quasi-isotropic strength *Composites A* **147** 106442
[36] Silk fibre composites WO2007110758
[37] Mosleh Y, Clemens D, Gorbatikh L, Verpoest I and Van Vuure A 2015 Penetration impact resistance of novel tough steel fibre-reinforced polymer composites *J. Reinf. Plast. Compos.* **34** 624–35
[38] Vanden Bosche K 2016 Development and characterization of novel anisotropic foam for bicycle helmets *PhD Thesis* Katholieke Universiteit Leuven, Leuven
[39] Mosleh Y, Vanden Bosche K, Rodriguez Perez M A, Vander Sloten J, Ivens J and Verpoest I 2013 Development of anisotropic foams and characterization methods for bicycle helmets (Composites week@Leuven)